

where $0 < c < 1$. After integrating over ϵ , one finds for the right-hand side

$$-\frac{kT e^{a/E_0}}{2\pi i} \int_{\epsilon-i\infty}^{\epsilon+i\infty} \frac{dZ \pi}{[\sin(\pi Z)(Z+kT/E_0)]} e^{Z(a-\zeta)/kT}. \quad (\text{A5})$$

Because $a-\zeta > 0$, we close the contour integral by a circle to the left in the complex Z plane. Summing up the contributions of all residues, one gets

$$I_1 - E_0 e^{a/E_0} = kT e^{a/E_0} \left(\frac{\pi e^{(\zeta-a)/E_0}}{\sin(\pi kT/E_0)} - \sum_{n=0}^{\infty} \frac{(-1)^n e^{-n(a-\zeta)/kT}}{kT/E_0 - n} \right). \quad (\text{A6})$$

One can easily see that the singularities on the right-

hand side of (A6) for $n \rightarrow kT/E_0$ cancel. Setting $\zeta = \zeta_{th}$, one finds, with $x = kT/E_0$,

$$I_1 = E_0 e^{\zeta_{th}/E_0} \left(\frac{\pi x}{\sin \pi x} - x e^{2x} \sum_{n=1}^{\infty} \frac{(-1)^n e^{-2n}}{x-n} \right). \quad (\text{A7})$$

Using (A6), one gets

$$I_2 = E_0 e^{\zeta_{th}/E_0} \left[\frac{\pi x^2}{\sin \pi x} - x e^{2x} \sum_{n=1}^{\infty} \frac{(-1)^n n e^{-2n}}{x-n} \right], \quad (\text{A8})$$

which can also be written as

$$I_2 = x I_1 - x E_0 e^{2x+\zeta_{th}/E_0} / (1+e^2). \quad (\text{A9})$$

The formulas (A7) and (A9) are used in a computer program to evaluate R_1 , R_2 , N_1 , and N_2 as functions of temperature.

Ultraviolet-Absorption Spectra of Europium and Ytterbium in Alkaline Earth Fluorides*

EUGENE LOH

Physical Sciences Department, McDonnell Douglas Astronautics Company, Western Division, Santa Monica, California 90406

(Received 3 February 1969)

The ultraviolet-absorption spectra of europium and ytterbium ions in CaF_2 crystals have been measured at room and liquid-nitrogen temperatures. Their spectra are similar to each other in the general location of their absorption bands. Both spectra consist of: (i) $4f \rightarrow 5d$ bands, between about $24\,000\text{ cm}^{-1}$ and about $50\,000\text{ cm}^{-1}$, due to isolated RE^{2+} with crystal field strength $\sim 17\,000\text{ cm}^{-1}$ between e_g and t_{2g} bands; (ii) $4f \rightarrow 5d$ bands, shifted $\sim 9\,000\text{ cm}^{-1}$ to higher energy, due to RE^{2+} ions surrounded by RE^{3+} neighbors; (iii) a $4f \rightarrow 6p$ broad and weak band of Eu^{2+} in CaF_2 with maximum at $\sim 71\,000\text{ cm}^{-1}$; and (iv) $4f \rightarrow 5d$ bands above $\sim 64\,000\text{ cm}^{-1}$ due to isolated RE^{3+} and cluster-ion RE^{3+} . The structure in the absorption spectra of both isolated $\text{RE}^{2+}(4f^n)$ and $\text{RE}^{3+}(4f^n)$ ions can be interpreted as formed through interaction between a $5d$ electron having e_g or t_{2g} crystal field symmetry and electrons in the ground multiplet of the $4f^{n-1}$ core.

I. INTRODUCTION

As a direct approach to the study of interconfigurational transitions of rare-earth (RE) ions in solids, we have previously presented the uv absorption spectra of two simple trivalent rare-earth ions, $\text{Ce}^{3+}(4f^1)$ (Ref. 1) and $\text{Pr}^{3+}(4f^2)$ (Ref. 2), in alkaline-earth fluorides. Their spectra show three types of transitions in the order of increasing energy: (a) $4f \rightarrow 5d$ bands, (b) a broad and weak $4f \rightarrow 6s$ band, and (c) the charge transfer of $\text{F}^-(2p^6) \rightarrow \text{RE}^{3+}(6s)$ appearing as the red shift of the absorption edge of the host crystal.

For comparison with the work on RE^{3+} , we present here the uv-absorption spectra of two common RE^{2+}

ions, $\text{Eu}^{2+}(4f^7)$ and $\text{Yb}(4f^{14})$, in CaF_2 . Contrary to most of RE ions in solids, europium and, to a lesser extent, ytterbium are usually in the divalent rather than trivalent state because of their tendency to complete the half, $\text{Eu}^{2+}(4f^7)$, and full, $\text{Yb}^{2+}(4f^{14})$, $4f$ shell, respectively. Their spectra are stable and perhaps also simple because no strenuous reduction process^{3,4} is required to convert RE^{3+} to RE^{2+} . Furthermore, the energy gaps in the ground multiplet of $4f^{n-1}$ are among the narrowest for Eu^{2+} , $4f^{n-1} = 4f^6$, and the widest for Yb^{2+} , $4f^{n-1} = 4f^{13}$. The uv-absorption spectra of Eu^{2+} and Yb^{2+} , therefore, provide simple examples to interpret the structure⁵ of $4f^n \rightarrow 4f^{n-1}5d$ bands and

* Work partially supported by the McDonnell Douglas Astronautics Company-Western Division under the Independent Research and Development Program.

¹ E. Loh, Phys. Rev. **154**, 270 (1967).

² E. Loh, Phys. Rev. **158**, 273 (1967).

³ J. L. Merz and P. S. Pershan, Phys. Rev. **162**, 217 (1967); **162**, 235 (1967); J. L. Merz, Ph.D. thesis, Harvard University, 1966 (unpublished). Available as Technical Report No. 514, Office of Naval Research, NR-372-012, and references therein.

⁴ D. S. McClure and Z. Kiss, J. Chem. Phys. **39**, 3251 (1963).

⁵ E. Loh, Phys. Rev. **175**, 533 (1968).

will be helpful in understanding complicated absorption spectra of other³⁻⁵ RE²⁺ in solids.

The spectrum of Eu²⁺ in CaF₂ shows two types of interconfigurational transitions: (a) 4*f* → 5*d* bands between 24 000 cm⁻¹ and 61 000 cm⁻¹ and (b) a 4*f* → 6*p* weak broad band with maximum at about 71 000 cm⁻¹. Occasionally in some europium-doped CaF₂ narrow bands dominate the spectral region above 62 000 cm⁻¹. These bands are interpreted as 4*f* → 5*d* bands of Eu³⁺ in CaF₂ (Refs. 5 and 6). The spectrum of ytterbium in CaF₂ is dominated by 4*f* → 5*d* bands of Yb²⁺ at low energy and that of Yb³⁺ above 66 000 cm⁻¹.

We shall interpret the 4*f* → 5*d* bands of both Eu²⁺ and Yb²⁺ as originating from both isolated RE²⁺ ions and RE²⁺ ions with RE³⁺ neighbors; and the 4*f* → 5*d* bands of Eu³⁺ and Yb³⁺ because of isolated RE³⁺ ions and cluster-ions RE³⁺ as in previous cases of Ce³⁺ (Ref. 1) and Pr³⁺ (Ref. 2). The structures in 4*f* → 5*d* bands of isolated RE²⁺ (4*fⁿ*) and RE³⁺ (4*fⁿ*) ions will be interpreted as formed by components of 5*d* orbitals, *e_g* or *t_{2g}*, interacting with ground multiplet of 4*fⁿ⁻¹* core.

Following our previous pattern^{1,2} on RE³⁺, this work is mainly concerned with the nature of the absorption bands rather than the assignment of individual levels. We first discuss the uv-absorption spectra of europium in CaF₂ and SrF₂ and then that of ytterbium in CaF₂.

II. ULTRAVIOLET ABSORPTION SPECTRA OF EU²⁺ IN CaF₂ AND SrF₂

The uv-absorption spectra of Eu²⁺ in CaF₂ are shown in Figs. 1 and 2, respectively. The two low-energy (<50 000 cm⁻¹) bands have been reported by Kaplyanskii and Feofilov⁷ and have been assigned as *e_g* and *t_{2g}* of a 5*d* orbital in the cubic crystal field. We assign all three bands below about 60 000 cm⁻¹ as 4*f* → 5*d* bands. Specifically, we interpret the two lower bands, centered at ~28 000 and ~45 000 cm⁻¹ in CaF₂ and at ~29 000 and ~44 000 cm⁻¹ in SrF₂, as *e_g* and *t_{2g}* bands of isolated Eu²⁺ in crystals; we speculate that there is a band hidden somewhere in or near the huge 44 000-cm⁻¹ band of both crystals. This hidden band and the weak band,⁸ which is centered at ~56 000 cm⁻¹ in CaF₂ and ~54 000 cm⁻¹ in SrF₂, are also interpreted as *e_g* and *t_{2g}* bands, respectively, of Eu²⁺ ion with Eu³⁺ as next nearest neighbors. This latter interpretation of Eu²⁺ ion with Eu³⁺ neighbors will be discussed together with the corresponding Yb²⁺—Yb³⁺ absorption in Sec. IV.

⁶ E. Loh, Phys. Rev. **147**, 332 (1966).

⁷ A. A. Kaplyanskii and P. P. Feofilov, Opt. i Spektroskopiya **13**, 235 (1962) [English transl.: Opt. Spectry. (USSR) **13**, 129 (1962)].

⁸ The location of this weak band in CaF₂:Eu²⁺ is higher than that in SrF₂:Eu²⁺, ~56 000 versus ~54 000 cm⁻¹. This is consistent with the assignment of *t_{2g}*, which is displaced to higher energy in a smaller host crystal.

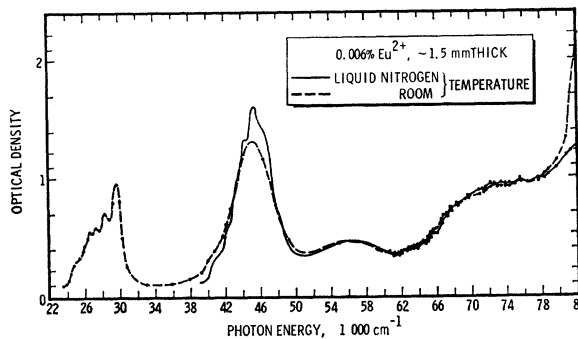


FIG. 1. Ultraviolet absorption spectrum of Eu²⁺ in CaF₂.

At energies higher than 62 000 cm⁻¹, CaF₂:Eu²⁺ shows a broad band centered at about 71 000 cm⁻¹ (see Fig. 1). This Eu²⁺ band is due to 4*f* → 6*p* transitions and not to 4*f* → 6*s*, as in the case of CaF₂:Ce³⁺ (Ref. 1) or CaF₂:Pr³⁺ (Ref. 2). The 4*f* → 6*p* assignment is based on two relevant comparisons: (i) between free-ion data⁹ of Eu²⁺ and Ce³⁺ (or Pr³⁺) and (ii) between relative strength of the 4*f* → 6*p* band versus the 4*f* → 6*s* band. First, the 4*f* → 6*p* centroid⁹ of free-ion Eu²⁺ is ~40 000 cm⁻¹ above the 4*f* → 5*d* centroid. This is close to the value⁹ of the 4*f* → 6*s* centroid minus the 4*f* → 5*d* centroid of free-ion Ce³⁺ or Pr³⁺, that is, about 35 000 cm⁻¹. Going from the free ion to the solid, we expect that the relative locations of the 4*f* → 6*p* and 4*f* → 5*d* bands of Eu²⁺ are also comparable to those of the 4*f* → 6*s* and 4*f* → 5*d* bands of Ce³⁺ (Ref. 1) or Pr³⁺ (Ref. 2). On the other hand, the 4*f* → 6*s* centroid of free-ion Eu²⁺ is only ~5 000 cm⁻¹ above the 4*f* → 5*d* centroid. This means the weak 4*f* → 6*s* band of Eu²⁺ in CaF₂ is likely hidden in the huge *t_{2g}* band centered at ~45 000 cm⁻¹, as shown in Fig. 1. Secondly, by visual comparison in Fig. 1, the relative strength of the 4*f* → 6*p* band, with respect to the 4*f* → 5*d* band of CaF₂:Eu²⁺, is greater than that of 4*f* → 6*s* band of CaF₂:Ce³⁺ (Ref. 1) or CaF₂:Pr³⁺ (Ref. 2). The 4*f* → 6*p* transition with $\Delta l = f - p = 3 - 1 = 2$ should be less

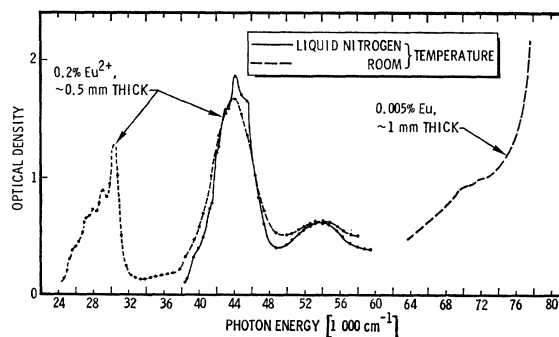


FIG. 2. Ultraviolet absorption spectrum of europium in SrF₂.

⁹ G. H. Dieke and H. M. Crosswhite, Appl. Opt. **2**, 675 (1963); G. H. Dieke, H. M. Crosswhite, and B. Dunn, J. Opt. Soc. Am. **51**, 820 (1961).

forbidden, therefore stronger, than the $4f \rightarrow 6s$ transition with $\Delta l = f - s = 3 - 0 = 3$.

The high-energy spectrum of Eu^{2+} in our $\text{SrF}_2:0.2\%$ Eu sample is unfortunately masked by large absorption due to other impurity and is therefore omitted at energies above $60\,000\text{ cm}^{-1}$, in Fig. 2.

We proceed to discuss briefly the structure in the $4f \rightarrow 5d$ bands of Eu^{2+} in CaF_2 and SrF_2 . Each hump in the lowest $4f \rightarrow 5d$ band shown in Figs. 1 and 2 can be interpreted as unresolved vibronics. In this $5d$ band, Kaplyanskii *et al.*^{7,10} have resolved the pure electronic transitions and some associated vibronics at liquid-helium temperature. The separations between pure electronic lines of Eu^{2+} are about the same^{10,7} in CaF_2 and SrF_2 and are approximately equal¹⁰ to the known intervals ${}^7F_{j+1} - {}^7F_j$ between the j levels of the 7F_j multiplets of Eu^{3+} . These electronic lines are therefore interpreted¹⁰ as transitions to states of $4f^6 5d$ generated by the interaction of the $5d(e_g)$ electron with various states of the ground multiplet of the $4f^6$ core, i.e., transitions to states $4f^6({}^7F_0)5d(e_g)$, $4f^6({}^7F_1)5d(e_g)$, \dots , $4f^6({}^7F_6)5d(e_g)$. The locations of these pure electronic transitions¹⁰ of Eu^{2+} in CaF_2 and SrF_2 are shown in Figs. 1 and 2, respectively, by vertical markers on the lowest band. Most of markers indeed precede the humps in the lowest $5d$ band at room temperature.

The t_{2g} band of isolated Eu^{2+} has also humps as shown by the liquid-nitrogen spectra in Figs. 1 and 2. The separations between humps are again about the same in both host crystals except for a uniform shift in energy, and they are approximately equal to those in the e_g band. By analogy, we speculate that the humps in the t_{2g} band of isolated Eu^{2+} in CaF_2 of Fig. 1 and SrF_2 of Fig. 2 are also unresolved vibronics, at liquid-nitrogen temperature, of transitions to $4f^6({}^7F_j)5d(t_{2g})$. Unfortunately, there is no corresponding 4.2°K data available in the literature for direct comparison. In order to demonstrate the feasibility of this interpretation, we have translated the entire set of markers from e_g band to t_{2g} band in both Figs. 1 and 2. The markers appear to precede prominent humps in the second lowest band.

Table I summarizes the data on $4f \rightarrow 5d$ and $4f \rightarrow 6p$ bands of Eu^{2+} in CaF_2 and SrF_2 . The energies are arbitrarily located at the band maxima, since, unfortunately, no structures can be observed in bands at energies above $50\,000\text{ cm}^{-1}$. Values of crystal-field strength, $10Dq$, obtained as the separation between the e_g and t_{2g} bands of isolated Eu^{2+} , are also listed in the table. They are larger than the corresponding values of about $12\,000\text{ cm}^{-1}$ in CaF_2 and about $11\,000\text{ cm}^{-1}$ in SrF_2 , as deduced from locations of $5d$ bands of single ion Ce^{3+} or Pr^{3+} in alkaline earth fluorides.^{1,2} The smaller size of the $5d$ orbital on the triply ionized

TABLE I. Approximate energies (cm^{-1}) of $4f \rightarrow 5d$, $4f \rightarrow 6p$ and crystal-field strength $10Dq$, of isolated Eu^{2+} ion in CaF_2 and SrF_2 .

Host crystal	Cubic		Centroid		Crystal-field strength, $10Dq$
	e_g	t_{2g}	$4f \rightarrow 5d$	$4f \rightarrow 6p$	
CaF_2	28 200	45 200 56 000 ^a	38 400	71 000	17 000
SrF_2	29 000	44 000 54 000 ^a	38 000		15 000

^a The corresponding assignment for Eu^{2+} ions with Eu^{3+} neighbors.

rare-earth ions may be responsible for the correspondingly smaller value of the crystal field strength.

III. ULTRAVIOLET ABSORPTION SPECTRA OF Eu^{3+} IN CaF_2 AND SrF_2

Although europium ions in alkaline-earth fluorides are usually divalent because of the half-shell effect, we found occasional evidence of strong absorption due to Eu^{3+} in CaF_2 . This is shown in the high-energy region, $>62\,000\text{ cm}^{-1}$, of the uv-absorption spectrum of $\text{CaF}_2:\text{Eu}$, Fig. 3. We assign the strong absorption peak at $68\,500\text{ cm}^{-1}$ as a $4f \rightarrow 5d(e_g)$ band of single-ion Eu^{3+} because its characteristics resemble those of other^{6,1,2} RE^{3+} ions in CaF_2 . These characteristics are: band width and its narrowing at low temperature (from $\sim 1400\text{ cm}^{-1}$ at room temperature to $\sim 900\text{ cm}^{-1}$ at liquid-nitrogen temperature); e_g -type red shift at low temperature; absorption cross section of the band $\sim 10^{-18}\text{ cm}^2$ and correct location⁶ of the band. Following the interpretation⁵ on the structure of Eu^{2+} absorption in Sec. II, we speculate that the peaks between $63\,000$ and $76\,000\text{ cm}^{-1}$ in Fig. 3 are due to $4f^6 \rightarrow 4f^5 5d(e_g)$ transitions formed by interaction of $5d(e_g)$ with the ground multiplets $4f^6({}^6H$ and ${}^6F)$ of single-ion Eu^{3+} in CaF_2 . A set of markers whose energy gaps are equal to those of the ground multiplets⁹ of the $4f^6$ core is placed at low-energy side of the Eu^{3+} peaks in Fig. 3 and demonstrates again the plausibility of this interpretation.⁵

Because of the dominance of the crystal-field effect on the $5d$ orbitals of RE, the separations between $4f \rightarrow 5d$ bands in the absorption spectra of Ce^{3+} (Ref. 1)

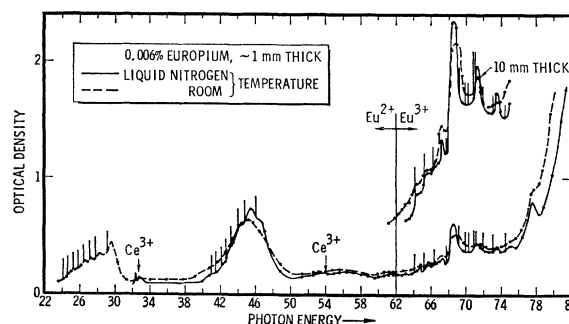


Fig. 3. Ultraviolet absorption spectrum of europium in CaF_2 .

¹⁰ A. A. Kaplyanskii and A. K. Przhvuskii, *Opt. i Spektroskopiya* **19**, 597 (1965) [English transl.: *Opt. Spectry.* (USSR) **19**, 331 (1965)].

are approximately equal to the corresponding gaps of Pr^{3+} (Ref. 2), Nd^{3+} (Ref. 11) and Sm^{3+} (Ref. 11), that is, independent of these RE^{3+} . If this similarity between $4f \rightarrow 5d$ absorption spectra of Ce^{3+} , Pr^{3+} , Nd^{3+} , and Sm^{3+} is extended to the spectra of Eu^{3+} in CaF_2 , the band at $77\,500\text{ cm}^{-1}$ in Fig. 3 is assigned as $4f \rightarrow 5d(e_g)$ absorption of cluster-ion Eu^{3+} and other $4f \rightarrow 5d$ bands are either on or beyond the absorption edge of the host CaF_2 at $\sim 81\,000\text{ cm}^{-1}$. The separation between the cluster-ion band at $77\,500\text{ cm}^{-1}$ and the single-ion peak at $68\,500\text{ cm}^{-1}$ is $9\,000\text{ cm}^{-1}$, which is equal to the corresponding separation in Ce^{3+} (Ref. 1) and Pr^{3+} (Ref. 2).

The Eu^{3+} absorption in $\text{SrF}_2:0.005\%\text{Eu}$ is shown in the high-energy region of Fig. 2. The room-temperature spectrum shows an excess absorption between $\sim 68\,500$ and $\sim 72\,500\text{ cm}^{-1}$ with two humps at $\sim 69\,800$ and $71\,800\text{ cm}^{-1}$. These two humps correspond with the two strong peaks of Eu^{3+} in CaF_2 , $\sim 68\,900$ and $\sim 71\,300\text{ cm}^{-1}$, respectively, at room temperature, in Fig. 3. The Eu^{3+} absorption shifts toward higher energies in SrF_2 from that in CaF_2 . This is consistent with the e_g assignment of the $5d$ orbital in the cubic crystal field, whose strength weakens in a larger lattice, SrF_2 .

IV. ULTRAVIOLET ABSORPTION SPECTRUM OF Yb^{2+} IN CaF_2

The uv absorption spectra of ytterbium in CaF_2 are shown in Figs. 4 and 5. They are dominated by Yb^{2+} and Yb^{3+} absorptions at energies below and above, respectively, $66\,000\text{ cm}^{-1}$. Yb^{2+} absorption will be discussed in this section and Yb^{3+} in the next. The samples used in Fig. 5 contain traces of Ce^{3+} and Pr^{3+} , as indicated by arrows in the spectra. The sample of Fig. 4 is free of Ce^{3+} and Pr^{3+} absorption. Following Kaplyanskii and Feofilov,⁷ we assign the first band at $27\,400\text{ cm}^{-1}$ as the lowest e_g band and the band with maximum at $44\,100\text{ cm}^{-1}$, at 77°K , as the lowest t_{2g} band of isolated Yb^{2+} in CaF_2 . Figures 4 and 5 show that the separation between these two bands, or $10Dq \approx 16\,700\text{ cm}^{-1}$, is about same as that of Eu^{2+} in Figs. 1 or 3; this separation decreases at room temperature. These observations support the e_g and t_{2g} assignment.

Following the interpretation⁵ of the structure in Eu^{2+} absorption, Sec. II, we assign the lowest peak at $27\,400\text{ cm}^{-1}$ as $5d(e_g)4f^{13}(^2F_{7/2})$ and the "twin peak" near $\sim 37\,800\text{ cm}^{-1}$ as $5d(e_g)4f^{13}(^2F_{5/2})$; their energy difference, $37\,800 - 27\,400 = 10\,400\text{ cm}^{-1}$, is close to that⁹ of $^2F_{5/2} - ^2F_{7/2}$. Similarly, the band with maximum at $44\,100\text{ cm}^{-1}$ and the shoulder at $\sim 54\,500\text{ cm}^{-1}$ at 77°K in Fig. 4 are assigned as $5d(t_{2g})4f^{13}(^2F_{7/2})$ and $5d(t_{2g}) - 4f^{13}(^2F_{5/2})$, respectively; the energy difference between these two assignments is again equal to $10\,400\text{ cm}^{-1} \approx ^2F_{5/2} - ^2F_{7/2}$ (Ref. 9). The twin peak at $37\,800\text{ cm}^{-1}$ is due to vibronics.⁷

In analogy with $\text{Eu}^{2+} - \text{Eu}^{3+}$ complex in CaF_2 and SrF_2 , there are also absorptions due to Yb^{2+} ions, which

¹¹ E. Loh (unpublished).

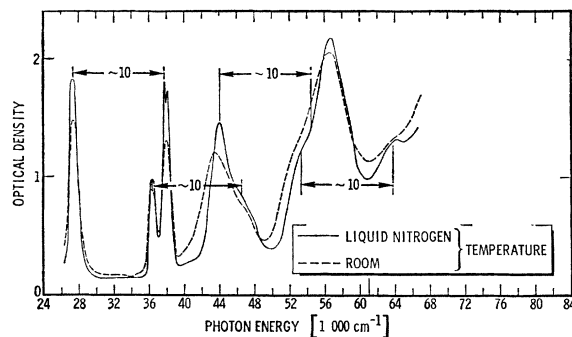


FIG. 4. Ultraviolet absorption spectrum of Yb^{2+} in CaF_2 .

are probably surrounded by Yb^{3+} ions. The $4f \rightarrow 5d$ assignments and the corresponding locations, in Fig. 4, of these Yb^{2+} ions are: (a) $4f^{13}(^2F_{7/2})5d(e_g)$ as a narrow band at $36\,400\text{ cm}^{-1}$ and $4f^{13}(^2F_{5/2})5d(e_g)$ as band shoulders at $46\,800\text{ cm}^{-1}$, with a separation of $46\,800 - 36\,400 = 10\,400\text{ cm}^{-1} \approx ^2F_{5/2} - ^2F_{7/2}$ between them. (b) $4f^{13}(^2F_{7/2})5d(t_{2g})$ as a band shoulder at $53\,100\text{ cm}^{-1}$ and $4f^{13}(^2F_{5/2})5d(t_{2g})$ as a hump at $63\,500\text{ cm}^{-1}$, with the separation of $63\,500 - 53\,100 = 10\,400\text{ cm}^{-1} \approx ^2F_{5/2} - ^2F_{7/2}$.

We may expect the characteristics of RE^{2+} ion with RE^{3+} neighbors as follows: (a) The $4f \rightarrow 5d$ energy of RE should increase in the following order, from (i) the isolated RE^{2+} ions to (ii) ER^{2+} ions with RE^{3+} neighbors and then to (iii) the isolated ER^{2+} ions, due to correspondingly increasing effective charge⁹ on the RE ions. (b) The absorption due to RE^{2+} ions with RE^{3+} neighbors relative to that of isolated RE^{2+} ions should be weaker for Eu than Yb in alkaline-earth halides, since Eu^{3+} ions are usually scarce in these hosts because of the half-shell effect of $\text{Eu}^{2+}(4f^7)$. Our interpretation on the $4f \rightarrow 5d$ absorption of Eu^{2+} ions with Eu^{3+} neighbors in Figs. 1–3 and of Yb^{2+} ions with Yb^{3+} neighbors in Figs. 4 and 5 are consistent with these characteristics. For RE ions other than Eu and Yb, we are unable to demonstrate the $f \rightarrow d$ absorption due to RE^{2+} ions with RE^{3+} neighbors clearly. Two complications may have masked such observations. First, the $4f^{n-1}$ ground multiplet, which constitutes the structure⁵ in the $4f^n \rightarrow 4f^{n-1}5d$ absorp-

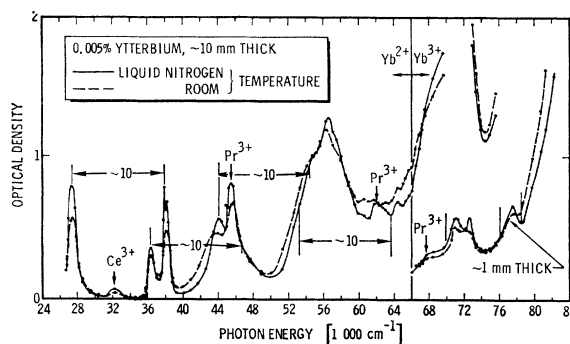


FIG. 5. Ultraviolet absorption spectrum of ytterbium in CaF_2 .

TABLE II. Approximate energies (cm^{-1}) of $4f^{14} \rightarrow 4f^{13}5d$ and crystal-field strength of isolated Yb^{3+} in CaF_2 and free ion Yb^{2+} .

$4f^{14}$	$4f^{13}5d$ Assignments		Centroid		Crystal-field strength, $10Dq$
	e_g	t_{2g}	Yb^{2+} in CaF_2	Free-ion Yb^{2+}	
${}^2F_{7/2}$	27 400	44 100	37 400		16 700
	36 400 ^a	53 100 ^a		44 100	
${}^2F_{5/2}$	37 800	54 500	47 820		16 700
	46 800 ^a	63 500 ^a			

^a The corresponding assignments for Yb^{2+} with Yb^{3+} neighbors.

tion bands, of most RE^{2+} ions has either a wider span than that of Eu^{2+} with $4f^{n-1} = 4f^6$ or more than two levels as in the case of Yb^{2+} with $4f^{n-1} = 4f^{13}$ (${}^2F_{7/2}$ and ${}^2F_{5/2}$). Secondly, the extra reduction process of $\text{RE}^{3+} \rightarrow \text{RE}^{2+}$, which is usually required to produce divalent ion of most RE in alkaline-earth halides, may introduce some defects to complicate further the environment around the RE^{2+} ions. A possible supporting evidence for the presence of the $\text{RE}^{2+} - \text{RE}^{3+}$ complex is the absorption behavior³ of RE^{2+} , e.g., Nd, Er, and Dy, in CaF_2 during the thermal bleaching. The RE^{2+} ions have been originally produced³ by x irradiation on the RE^{3+} -doped CaF_2 at 77°K . In the process of reconverting RE^{2+} back to RE^{3+} by warming up in steps to 300°K , the RE^{2+} absorptions in intermediate spectral regions³ do not decrease as steadily as in the other regions. The absorption in the former regions could originate from RE^{2+} ions with neighbors of RE^{3+} ions, which grow in number at increasing annealing temperatures.

Table II summarizes the experimental data and the assignments of $4f^{14} \rightarrow 4f^{13}5d$ of Yb^{2+} in CaF_2 . The $4f^{13}5d$ centroid of isolated Yb^{2+} ion in CaF_2 is shown at $\sim 42\,610\text{ cm}^{-1}$, which is only $\sim 4\%$ below the free-ion¹² value at $\sim 44\,100\text{ cm}^{-1}$. Table II also shows that the crystal-field strength, $10Dq$, on Yb^{2+} in CaF_2 , $\sim 16\,700\text{ cm}^{-1}$, is comparable⁷ to that on Eu^{2+} in CaF_2 , $\sim 17\,000\text{ cm}^{-1}$ in Table I.

For the free ion of Yb^{2+} (Refs. 9 and 12), the centroid of $4f \rightarrow 6s$ and $4f \rightarrow 6p$ are $\sim 5000\text{ cm}^{-1}$ lower and $\sim 37\,000\text{ cm}^{-1}$ higher, respectively, than that of $4f \rightarrow 5d$. We have failed to observe a well-defined $4f \rightarrow 6s$ band, which might occur in the visible region,^{7,13} in heavily doped,¹¹ $\sim 5\%$ and 20% Yb, CaF_2 crystals. The $4f \rightarrow 6p$ band of Yb^{2+} in CaF_2 is probably located near that of Eu^{2+} , with maximum at $\sim 71\,000\text{ cm}^{-1}$, as shown in Fig. 1. This band is therefore likely hidden in the absorption spectra of Yb^{3+} .

The large peak at $\sim 56\,400\text{ cm}^{-1}$ in $\text{CaF}_2:\text{Yb}$, Figs. 4 and 5, is probably because of defects associated with Yb doping. There are similar peaks¹¹ at $\sim 55\,000$ and

$\sim 49\,300\text{ cm}^{-1}$ in ${}^{60}\text{Co}$ irradiated $\text{SrF}_2:0.5\%$ Yb and $\text{BaF}_2:0.5\%$ Yb, crystals, respectively. It is interesting to note that this unknown defect level becomes shallower in larger crystals which have narrower energy gap between valence and conduction band.

V. ULTRAVIOLET-ABSORPTION SPECTRUM OF Yb^{3+} IN CaF_2

The uv-absorption spectrum of Yb^{3+} in CaF_2 is shown in Fig. 5 at energies above $\sim 66\,000\text{ cm}^{-1}$, except for one hump marked as absorption due to Pr^{3+} . Following the interpretation on the structure of Eu^{3+} absorption, the structures between $\sim 68\,000$ and $\sim 81\,000\text{ cm}^{-1}$ are due to $5d(e_g)4f^{12}({}^3H_6)$, $5d(e_g)4f^{12}({}^3H_4)$, and $5d(e_g)4f^{12}({}^3H_5)$ are led by three corresponding markers in Fig. 5. These markers have energy gaps equal to that in the ground multiplet of the $4f^{12}({}^3H)$ core.

VI. CONCLUSION

The interconfigurational absorption spectra of europium and ytterbium in CaF_2 are the simplest among all RE^{2+} ions because of the half-shell and full-shell effects, respectively. The spectra of these two ions are similar to each other, including the general location of the absorption bands. Both spectra consist of: (i) $4f \rightarrow 5d$ bands of isolated RE^{2+} with crystal-field strength $\sim 17\,000\text{ cm}^{-1}$ and $4f \rightarrow 5d$ band at higher energy due to RE^{2+} ions surrounded by RE^{3+} neighbors, (ii) a $4f \rightarrow 6p$ broad and weak band of Eu^{2+} in CaF_2 with maximum at $\sim 71\,000\text{ cm}^{-1}$, and (iii) $4f \rightarrow 5d$ bands above $\sim 64\,000\text{ cm}^{-1}$ due to isolated RE^{3+} and cluster-ion RE^{3+} , as in cases of Ce^{3+} and Pr^{3+} . The structure in the absorption spectra of both isolated $\text{RE}^{2+}(4f^n)$ and $\text{RE}^{3+}(4f^n)$ can be interpreted as formed through interaction between $5d$ electron, e_g or t_{2g} , with that in the ground multiplet of $4f^{n-1}$ core.

ACKNOWLEDGMENTS

The author is grateful to Hughes Research Laboratories, where the vacuum uv measurements were performed. He is indebted to the late beloved G. Dorosheski for the tireless computation and construction of numerous graphs and R. R. Carlen for some optical measurements. He also wishes to thank D. Rusling of Northrop Corp. Laboratories for ${}^{60}\text{Co}$ irradiation on some Yb-doped samples, L. Clark of University of California at San Diego for the permission of using double-beam vacuum uv spectrometer, and J. Merz, now at Bell Telephone Laboratories, and U. Ranon for discussions. Crystals were supplied by Optovac, Inc. J. R. Henderson has kindly read the manuscript. This work is partially supported by the Douglas Independent Research and Development (IRAD) program.

¹² B. W. Bryant, J. Opt. Soc. Am. **55**, 771 (1965).

¹³ P. P. Feofilov, Opt. i Spektroskopiya **1**, 992 (1956).